Responsive Polymer-Based Assemblies for Sensing Applications

Xue Li, Yongfeng Gao, Michael J. Serpe*

Department of Chemistry, University of Alberta, Edmonton, Alberta, Canada

*Corresponding Author -- michael.serpe@ualberta.ca

Abstract:

Poly (N-isopropylacrylamide) (pNIPAm)-based hydrogels and hydrogel particles (microgels) have been extensively studied since their discovery and "popularization" a few decades ago. While their uses seem to have no bounds, this feature article is focused on their development and application for sensing small molecules, macromolecules, and biomolecules. We highlight hydrogel/microgel-based photonic materials that have order in one, two, or three dimensions, which exhibit optical properties that depend on the presence and concentration of various analytes.

Keywords: stimuli-responsive polymer; photonic materials; poly (N-isopropylacrylamide)-based microgels; etalons; optical sensing

Introduction:

Polymer-based stimuli responsive materials have been of great interest over the years due to their ability to convert external chemical or physical stimuli into observable changes of the material itself.[1-3] Some of the most important of these materials are responsive hydrogels, which are hydrophilic crosslinked polymer networks capable of changing their solvation state in response to various stimuli.[4-6] Some of those stimuli include temperature,[7, 8] light,[9, 10] electric,[11] and magnetic fields.[12] These responsivities make hydrogels very useful for sensing,[13, 14] drug delivery,[15, 16] and artificial muscles.[17, 18] Hydrogel particles (microgels) can also be synthesized, and can have diameters of 100 - 2000 nm.[19, 20] Poly (N-isopropylacrylamide) (pNIPAm)-based hydrogels and microgels are the most widely studied stimuli responsive polymers to date.[21-23] It is well known that pNIPAm is fully soluble in water below ~32^{o}C, and transitions to an "insoluble" state when the temperature is above 32^{o}C. This transition is observed as a coil-to-globule transition,

where the polymer transitions from an extended to collapsed state, respectively.[24] As a result, the crosslinked network of pNIPAm-based hydrogels and microgels likewise contract upon heating, and swell with water upon cooling.[25-27] This swelling-deswelling transition is fully reversible over multiple cycles.

While there are many uses of pNIPAm hydrogels and microgels, a majority of this review focuses on their use for sensing applications. Specifically, this review focuses on the use of microgels and hydrogels as optical components in photonic materials (PMs). A specific example of a PM is a photonic crystal (PC); PCs are composed of materials of varying refractive indices arranged in an ordered fashion in one, two, or three dimensions (1D, 2D, 3D). There are many examples of PCs in nature, most commonly associated with the vibrant colors of butterfly wings and the opal gemstone. These materials are unique because, unlike many other colored materials found in nature that exhibit color due to the absorbance of light by small molecule chromophores, they are colored due to their structure. Specifically, the opal gemstone is composed of a close-packed array of colloids (typically silica), which are capable of interacting with wavelengths of light in the visible region of the electromagnetic spectrum. These interactions lead to constructive and destructive interference of the light in the assembly, leading to specific wavelengths of light being reflected, which leads to the observed color.[28] To mimic the optical properties of opals, man made colloidal crystals have been a target research area in groups worldwide over many years. Most typically, colloids of high refractive index are "forced" into an ordered array in a matrix of relatively low refractive index. If the particle periodicity (i.e., refractive index periodicity) is on the order of visible wavelengths, then the device will appear colored. This is a direct result of light refraction, reflection, diffraction of the material's particles, which leads to light interference, and hence the color.[28-30] PM and PCs are of great interest in applications such as actuators,[31, 32] solar cells,[33, 34] and imaging.[35-37]

In this submission, we discuss recent examples of photonic materials with order in various dimensions. We highlight their fabrication and applications. The initial part of the submission is mainly focused on inorganic material, and block copolymer-based photonic materials, while the latter part of the submission focuses pNIPAm-based photonic materials that have been developed in the Serpe Group.

Colloidal crystals embedded in a functional/responsive polymer matrix emerged early on as interesting and appealing structures for sensing.[28] The Asher group has pioneered this research, calling these materials crystalline colloidal array (CCAs).[38] To accomplish this, they determined conditions required to self assemble colloids into a close packed array, which could be entrapped in a pNIPAm matrix. The resultant materials could change color in response to temperature changes. This is a direct result of the pNIPAm-based matrix changing volume, which changes the spacing between the array's optical elements. As mentioned, the assemblies exhibit Bragg-like diffraction, according to equation 1;

$$m\lambda = 2nd \sin\theta \qquad (1)$$

where m is the order of diffraction, λ is the wavelength of incident light, n is the refractive index of the suspension, d is the interplanar spacing, and θ is the glancing angle between the incident light and the diffracting crystal planes, which are oriented parallel to the crystal surface in the CCA they prepare. Figure 1 shows that the diffracted wavelength for the prepared polymerized crystalline colloidal array (PCCA) film could be tuned between 704 and 460 nm by variation in the temperature.

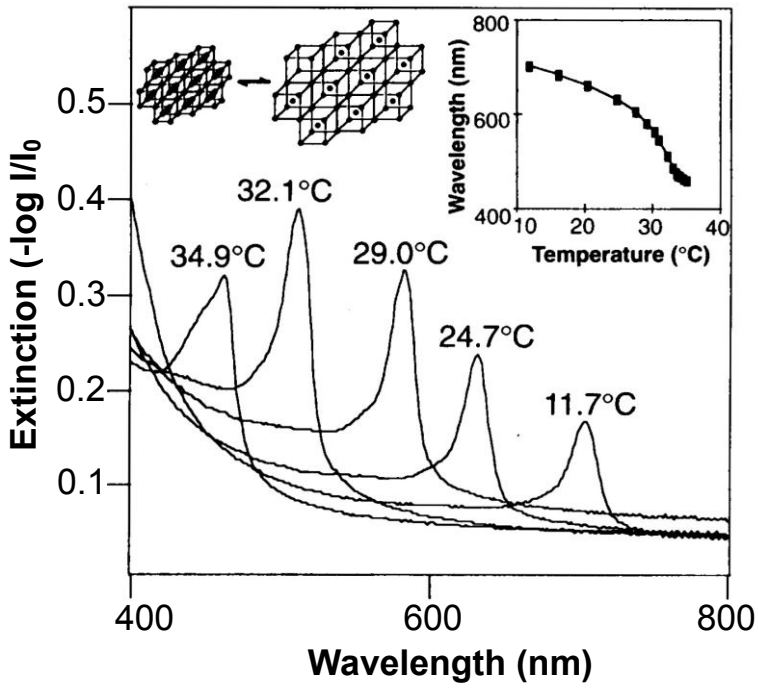

Figure 1. Temperature tuning of Bragg diffraction from a 125-μm-thick PCCA film of 99-nm PS spheres embedded in a pNIPAm gel. The shift of the diffraction wavelength results from the temperature-induced volume change of the gel, which alters the lattice spacing. Spectra were recorded in a UV-visible-near IR spectrophotometer with the sample placed normal to the incident light beam. The inset shows the temperature dependence of the diffracted wavelength for this PCCA film when the incident light is normal to the (110) plane of the lattice. Reprinted with the permission from [38] Copyright © 1996, American Association for the Advancement of Science.

In subsequent work, Asher and coworkers entrapped CCAs in various hydrogel materials, which changed volume (and hence optical properties) in the presence of various analytes, and upon exposure to a variety of stimuli.[6, 39, 40] In a recent example, the Asher group developed a novel two-dimensional (2D) crystalline colloidal array for the visual detection of amphiphilic molecules in water.[41] These 2D photonic crystals were placed on a mirror (a liquid Hg surface), and exhibited intense diffraction that enables them to be used for visual determination of analytes. Figure 2 is a schematic illustration of the 2D photonic crystal. A monolayer of 2D close-packed polystyrene (PS) particles was embedded in a pNIPAm-based hydrogel film. Binding of surfactant molecules

attaches ions to the sensor that swells the pNIPAm-based hydrogel. The resulting increase in particle spacing red shifts the 2D diffracted light. The 2D array Bragg diffraction condition is:

$$m\lambda = 3^{1/2} \times d \sin \theta \quad (2)$$

where m is the diffraction order, λ is the wavelength of the diffracted light, d is the nearest neighboring particle spacing, and θ is the angle between the incident light and the normal to the 2D array. For a fixed incidence angle θ, the diffracted wavelength, λ, is proportional to the 2D particle spacing, d. As shown in Figure 3, normalized and smoothed diffraction spectra of 2D pNIPAm-based sensors were obtained at different concentrations of aqueous, sodium dodecyl sulfate (SDS) solutions and diffraction wavelengths versus different concentration of SDS.

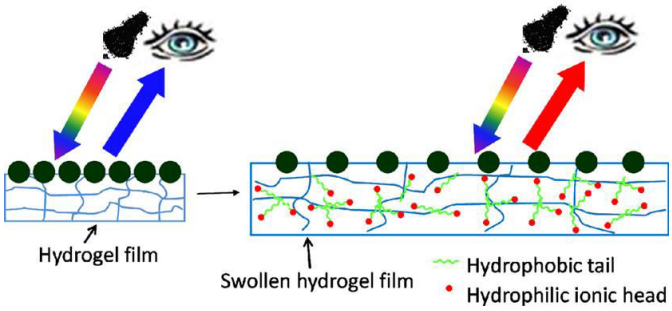

Figure 2. Schematic illustration of a 2D photonic crystal sensor formed by polymerization of a pNIPAm hydrogel network onto a 2D array of 490 nm PS particles on a liquid Hg surface. The pNIPAm hydrogel swells upon binding of surfactant molecules. The 2D particle spacing increases upon swelling of the pNIPAm hydrogel, red shifting the diffracted wavelength. Reprinted with the permission of [41] Copyright © 2012, American Chemical Society.

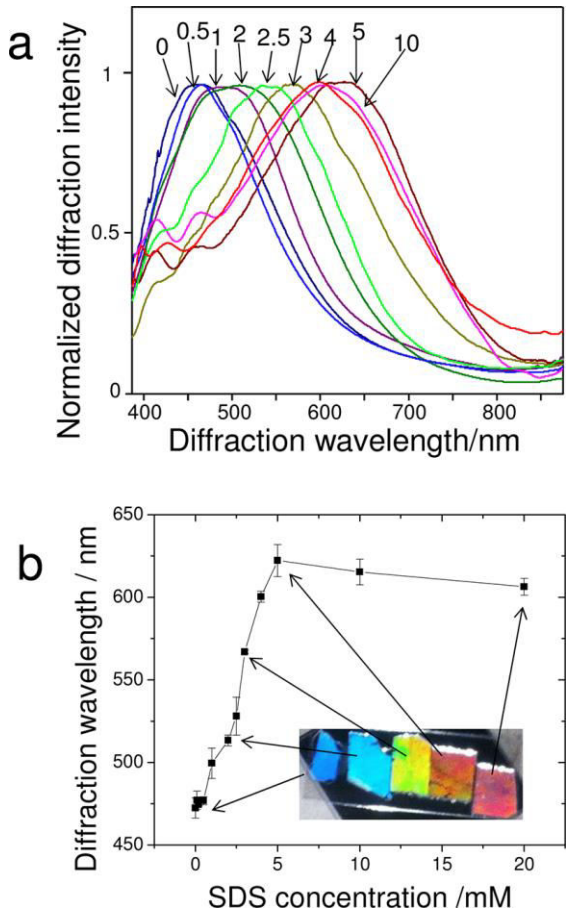

Figure 3. a, Normalized and smoothed diffraction spectra of 2D pNIPAm sensors at different concentrations of aqueous SDS solutions. Each number in the graph means the different concentration in the unit of mM. The spectra were measured with 40 ms accumulations. The measurement angle between the probe and the normal to the 2D array is 28°; b, Diffraction wavelength versus SDS concentration. The inset shows photographs taken close to the Littrow configuration at an angle of 28° between the source and camera to the 2D array normal. Reprinted with the permission of [41] Copyright © 2012, American Chemical Society.

In another example, Fudouzi and coworkers developed an elastic poly(dimethylsiloxane) (PDMS) sheet embedded with a thin layer of cubic close packed colloidal particles, which yielded tunable structural color.[42] Figure 4a shows that the sheet can be stretched horizontally and therefore the size is reduced in the vertical direction leading to the decrease in the lattice distance of (111) planes

of the array, then the blue shift of the reflectance peaks and the color change of the sheet, as shown in Figure 4b and c. Due to the ability of the devices to change color with elongation, it has potential applications for quantifying mechanical strains on materials, which could have use in monitoring the fidelity of building structures, bridges, etc.

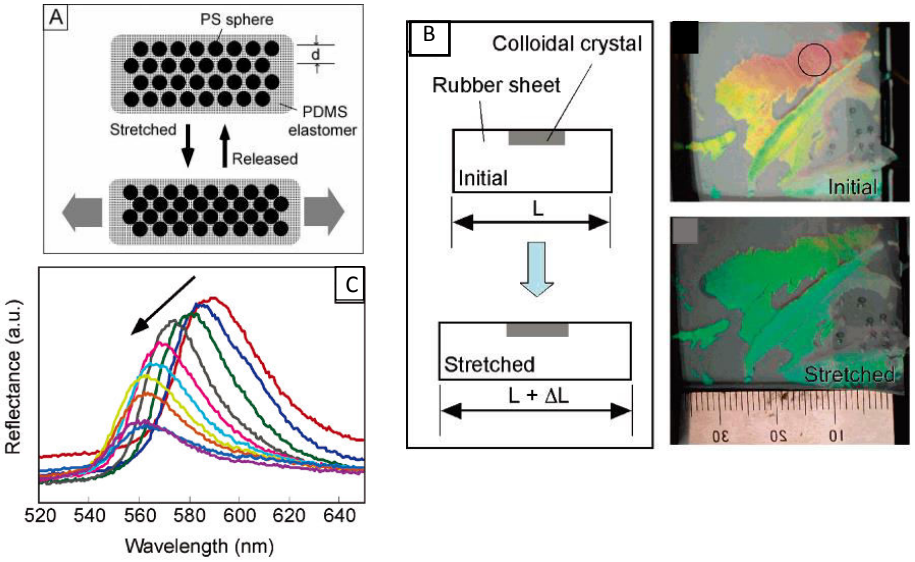

Figure 4. A, Reversible tuning by stretching of the lattice distance of a PS colloidal crystal embedded in a PDMS elastomer matrix; B, Changes in the structural color of the colloidal crystal film covering the silicone rubber sheet; C, Relationship between the reflectance peak position and elongation of the silicone rubber sheer by stretching. The peak position shifted from 590 to 560nm, and the reflectance intensity decreased gradually as indicated by the arrow. Reprinted with the permission of [42] Copyright © 2006, American Chemical Society.

Recently, there has been also a growing interest in using block copolymer photonic gels for biosensing applications. Block copolymers offer the flexibility of fabricating 1D, 2D and 3D photonic materials through self-assembly. Some photonic gels are extremely sensitive to changes in charges, as well as the dielectric environment; and for that matter, proteins, being highly charged dielectric materials, the electrostatic and dielectric environment of the photonic gels change abruptly upon protein binding. This property has been harnessed by the modification of photonic

gels with probe molecules and has been used for protein sensors transducing the binding of protein to the strong optical signals. Kang and coworkers[43] have realized this by using polystyrene-b-quaternized poly(2-vinyl pyridine) (PS-b-QP2VP) photonic gels modified with biotin molecules for detecting streptavidin. This was achieved by on-gel (Figure 5A) and in-gel (Figure 5B) modification with biotin via conventional carbodiimide coupling. An apparent visual color change with streptavidin binding was observed for the in-gel photonic materials, as shown in Figure 6.

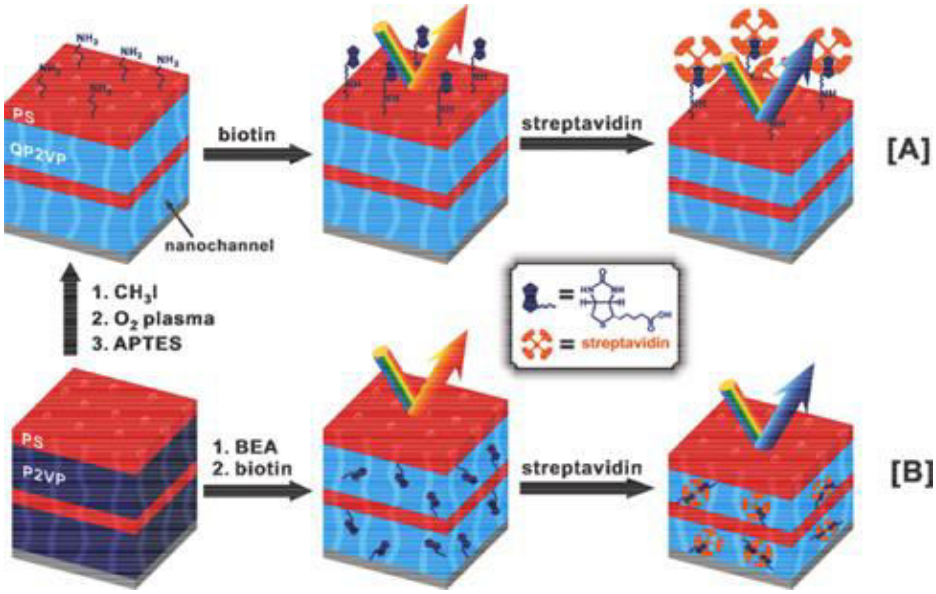

Figure 5. Preparation and the use of biotinylated photonic gels. A, procedure for surface modifying photonic gel films; B, procedure for preparing inside-biotinylated photonic gel films surface-modified photonic gel films. Reprinted with the permission of [43] Copyright © 2012, The Polymer Society of Korea and Springer Science+Business Media Dordrecht.

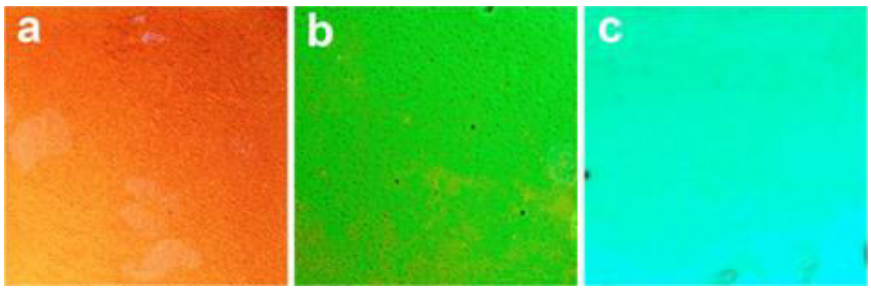

Figure 6. Color changes of the inside-biotinylated photonic gels in response to streptavidin; a, [S]=0 M; b, [S]=0.5 Mm; c, [S]=10 mM. Reprinted with the permission of [43] Copyright © 2012, The Polymer Society of Korea and Springer Science+Business Media Dordrecht.

Compared with other pNIPAm microgel-based photonic materials, which exhibit order in 2D or 3D,[41, 44, 45] our group recently designed a color tunable material (etalon) that exhibits order in 1D. This was accomplished by sandwiching a pNIPAm microgel-based layer between two thin Au layers, which act as mirrors. The devices exhibit visible color, and unique multipeak reflectance spectra -- the position of the peaks in the reflectance spectra primarily depend the thickness of the microgel layer, according to equation (3),

$$m\lambda = 2nd\cos\theta \qquad (3)$$

where m is the peak order; n is the refractive index of the dielectric material, d is the distance between Au layers, and θ is the angle of incidence.[46, 47] The structure of the device and representative reflectance spectra are shown in Figure 7. Since the optical properties depend on the thickness of the microgel layer (controls the mirror-mirror distance), the microgel's response to a stimulus results in changes in the optical properties.[48-54] This property is extremely important for sensing applications, since the solvation state of microgels can be made to depend on many different stimuli.

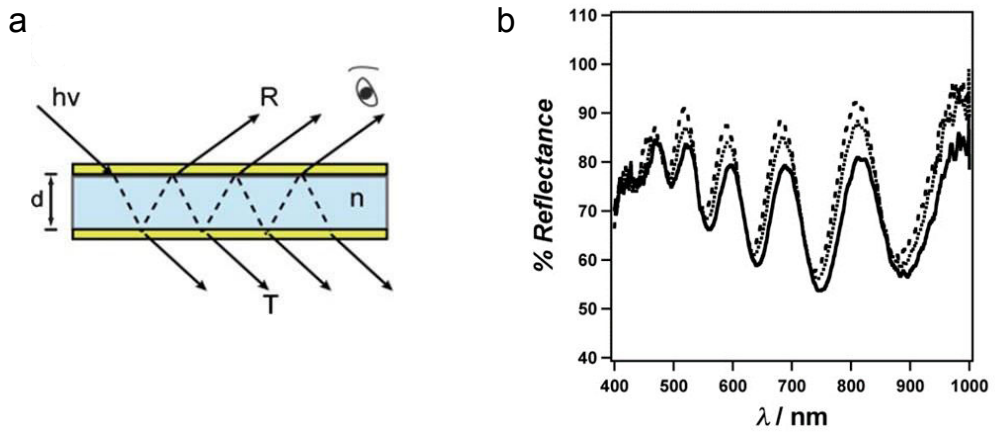

Figure 7. a, Structure of the microgel-based etalon. Two reflective metal (in this case Au) layers sandwiching a dielectric; b, Reflectance spectra from a typical pNIPAm microgel-based etalon. Reprinted with the permission of [49] Copyright © 2012, Royal Society of Chemistry.

In the most basic device iteration, the microgel solvation state depends on temperature, collapsing in water at T > ~ 32°C. This leads to a decrease in the thickness of the microgel layer, and hence equation 3 predicts a blue shift in the device's reflectance peaks. As can be seen in Figure 8, the device's reflectance peaks show a blue shift (e.g., the star-labelled peak) with increasing temperature in aqueous solution. This is due to microgel deswelling, resulting in the decrease of the distance between the device's Au layers.[55]

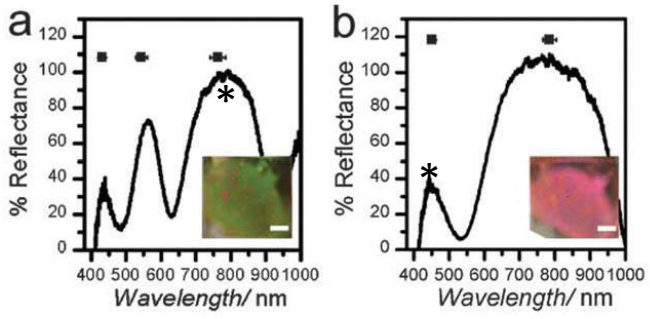

Figure 8. Representative spectra for an etalon in pH 3 solution (2 mM ionic strength (I.S.), I.S. adjusted with NaCl) at (a) 25°C, (b) 37°C. The insets show the corresponding photographs of the devices. Reprinted with the permission of [55] Copyright © 2013, Royal Society of Chemistry.

By copolymerizing acrylic acid (AAc) (pK_a ~ 4.25) with NIPAm, pH responsive pNIPAm-co-AAc microgels and microgel-based etalons could be achieved. This pH sensitive behavior is a result of Coulombic repulsion and osmotic swelling in the microgel layer at pH > pKa as a result of the deprotonated AAc groups. Furthermore, we sought to determine if spatially isolated regions of pNIPAm-co-AAc microgel-based etalons can be independently modulated.[49] Figure 9 shows an etalon with solutions of different pH spotted on spatially isolated regions. As can be seen, the spots appear different colors, which can be changed as a function of temperature and pH, independently. In another example, we have shown that pNIPAm-co-AAc microgel-based etalons could be attached to the surface of a quartz crystal microbalance, and used for the very sensitive detection of solution pH. [50, 56]

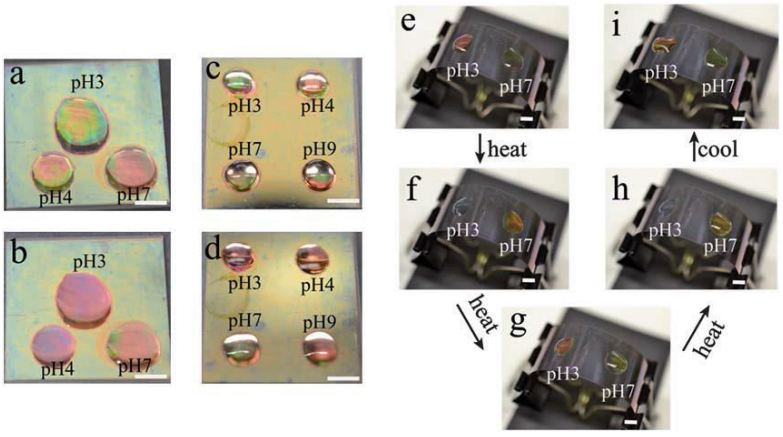

Figure 9. Photographs of an etalon with solutions of various pH spotted on a single surface (a, c, e, i) 25°C and (b, d, f, g, h) 37°C; (f) ~3 min after heating; (g) ~5 min after heating; (h) ~6 min after heating. In each panel, the scale bar is 5 mm. Reprinted with the permission of [49] Copyright © 2012, Royal Society of Chemistry.

Microgel-based etalons were also fabricated that could detect the concentration of glucose in solution. This was done by fabricating 3-aminophenylboronic acid (APBA) functionalized microgels.[48] As illustrated in Figure 10, glucose binding with the boron atom will promote more boron atoms to become negatively charged resulting in swelling of the microgel layer. Because λ

is proportional to the distance between the two mirrors, d, the swelling of microgels gives rise to a red shift of the reflectance peaks.

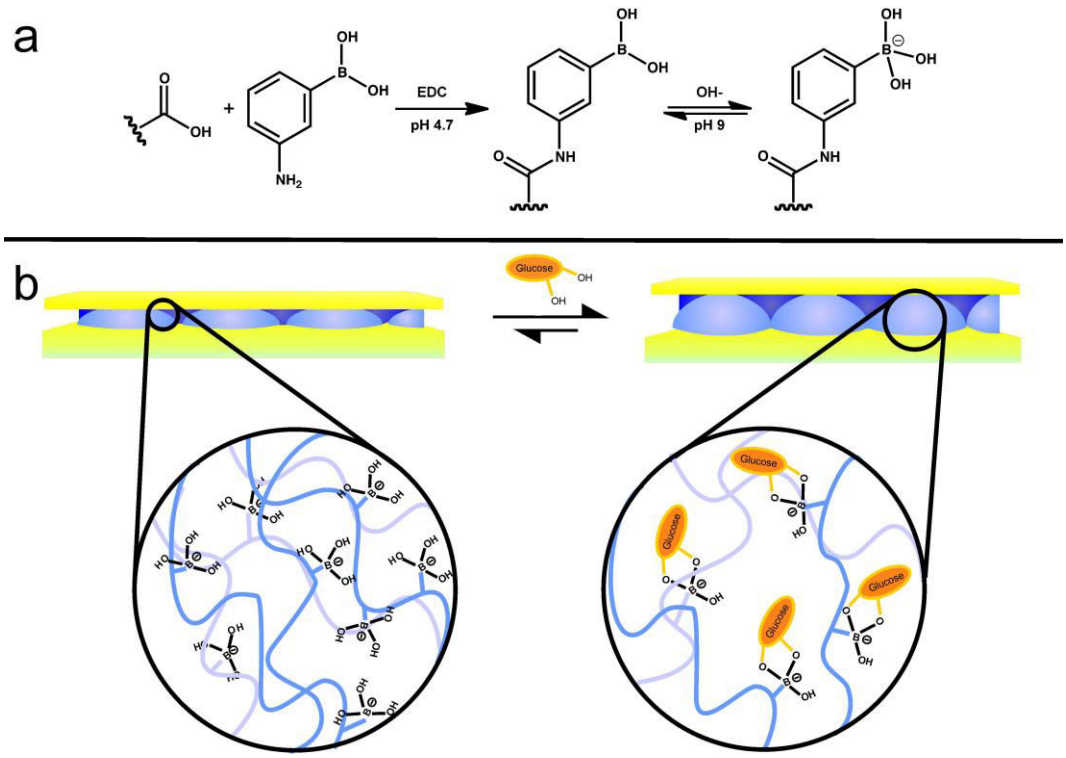

Figure 10. Reaction scheme for (a) the functionalization of the acrylic acid moieties on the microgel with 3-aminophenylboronic acid (APBA) followed by the activation of the boronic acid at high pH and (b) a cartoon depiction of the glucose responsivity of an APBA functionalized microgel etalon at pH 9. Reprinted with the permission of [48] Copyright © 2012, SpringerVerlag.

Etalons composed of either pNIPAm-co-AAc or pNIPAm-co-N-(3-aminopropyl)methacrylamide hydrochloride (pNIPAm-co-APMAH) microgels were also constructed.[57] We investigated their response to the presence of linear polycations and/or polyanions. When the etalon was at a pH that renders the microgels multiply charged, the microgel layer of the etalon deswells in the presence of the oppositely charged linear polyelectrolyte; it is unresponsive to the presence of the like charged polyelectrolyte. Furthermore, the etalon's response depended on the thickness of the Au overlayer. For example, low molecular weight (MW) polyelectrolyte could penetrate all Au overlayer thicknesses, while high MW polyelectrolytes could only penetrate the etalons fabricated from thin

Au overlayers, as shown in Figure 11a. We hypothesize that this is due to a decrease in the Au pore size with increasing thickness, which excludes the high MW polyelectrolytes from penetrating the microgel-based layer. Figure 11b shows the shift of λ for pNIPAm-co-AAc etalons in pH 6.5 solution after addition of poly(diallyldimethylammonium chloride) (pDADMAC) solution of different molecular weights (MW). From this observation, we then developed pNIPAm microgel-based etalons and etalon arrays to determine the molecular weights of polymers in solution.[58] These devices show promise as MW selective sensors and biosensors.

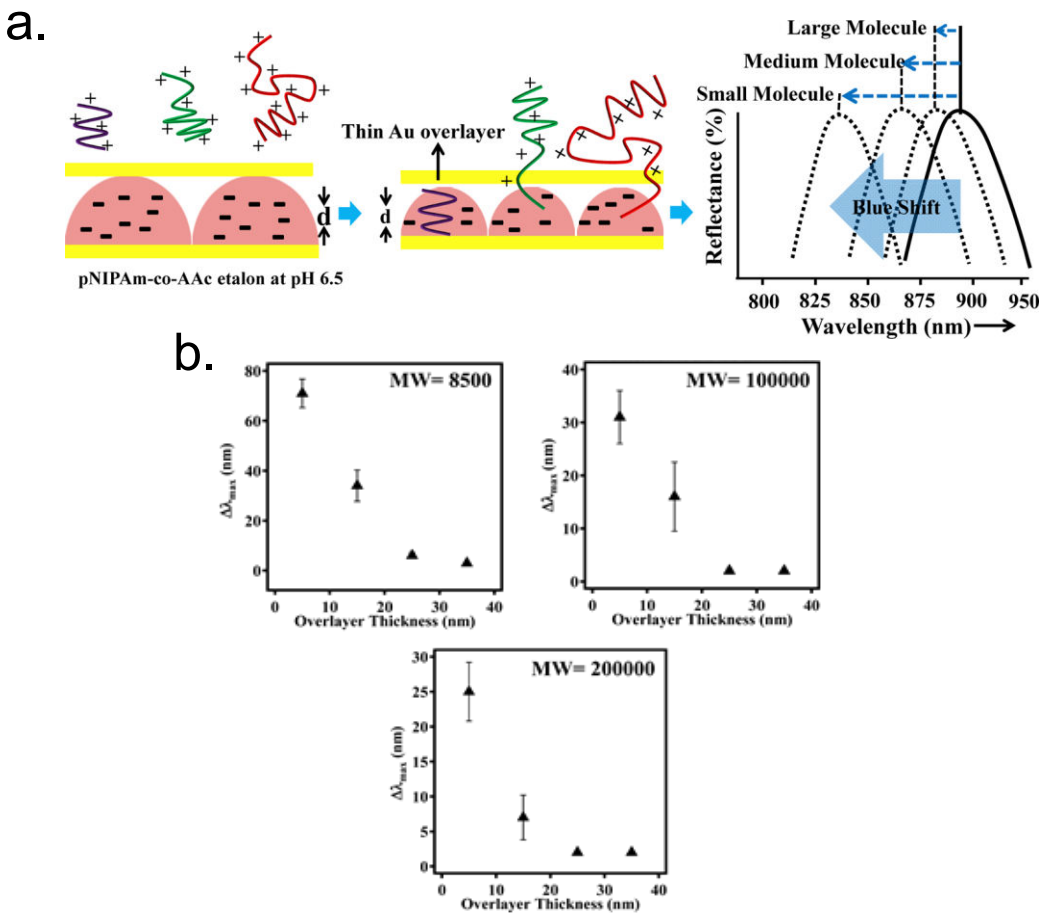

Figure 11. a, Schematic depiction of polyelectrolyte penetration through the porous Au overlayer of an etalon; b, Shift of λ_{max} for pNIPAm-co-AAc etalons in pH 6.5 after addition of pDADMAC solution with MW 8500, <100 000, and 100 000−200 000. Reprinted with the permission of [57] Copyright © 2013, American Chemical Society.

Based on our findings above that a polycationic polyelectrolyte can penetrate through the Au overlayer to interact with negatively charged microgel confined between Au overlayers, in subsequent studies we reported that biotinylated polycationic polymer can penetrate through the Au overlayer of a poly (N-isopropylacrylamide)-co-acrylic acid (pNIPAm-co-AAc) microgel-based etalon and cause the microgel layer to collapse.[51, 59] The collapse results in a shift in the spectral peaks of the reflectance spectra. We found that the extent of peak shift depends on the amount of biotinylated polycation added to the etalon, which can subsequently be used to determine the concentration of streptavidin in solution at pM concentrations. The sensing mechanism is shown in Figure 12.

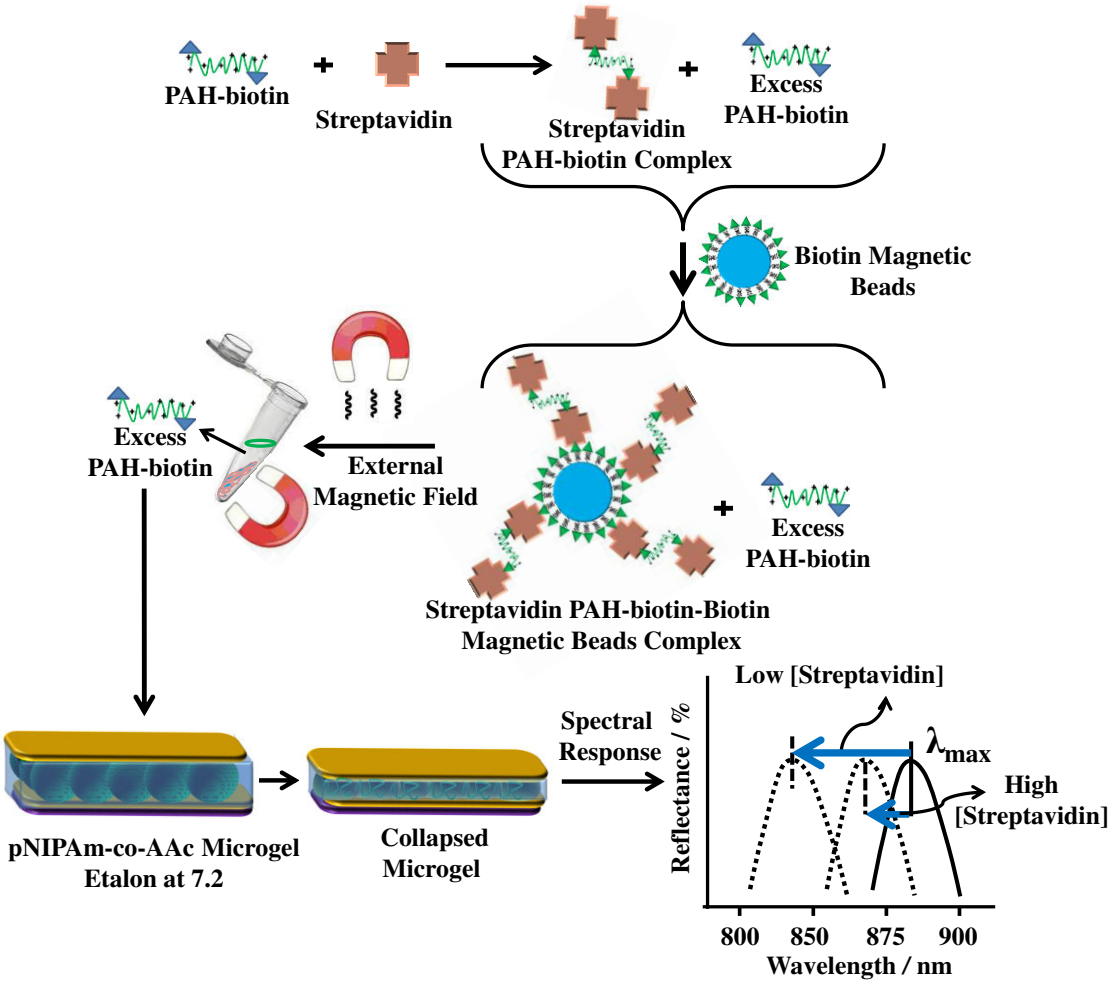

Figure 12. The proposed sensing mechanism. Streptavidin (the analyte) is added to an excess amount of biotin-modified poly (allylamine hydrochloride) (PAH). The streptavidin–biotin–PAH

complex is then removed from solution using biotin modified magnetic particles, leaving behind free, unbound PAH. The unbound PAH is subsequently added to a pNIPAm-co-AAc microgel-based etalon immersed in aqueous solution at a pH that renders both the microgel layer and the PAH charged. As a result, the etalon's spectral peaks shift in proportion to the amount of PAH–biotin that was added. This, in turn can be related back to the original amount of streptavidin added to the PAH–biotin. Reprinted with the permission of [59] Copyright © 2013, Elsevier.

As shown in Figure 13, the blue shift in the spectral peaks depends on the amount of streptavidin, and hence PAH-biotin, added to the etalon. We were able to detect streptavidin concentrations in the nM range without any system optimization. We also note that this response is unique due to the fact that the response is highest for the lowest streptavidin concentration -- this is counterintuitive based on the fact that other analytical approaches show small responses for low analyte concentrations.

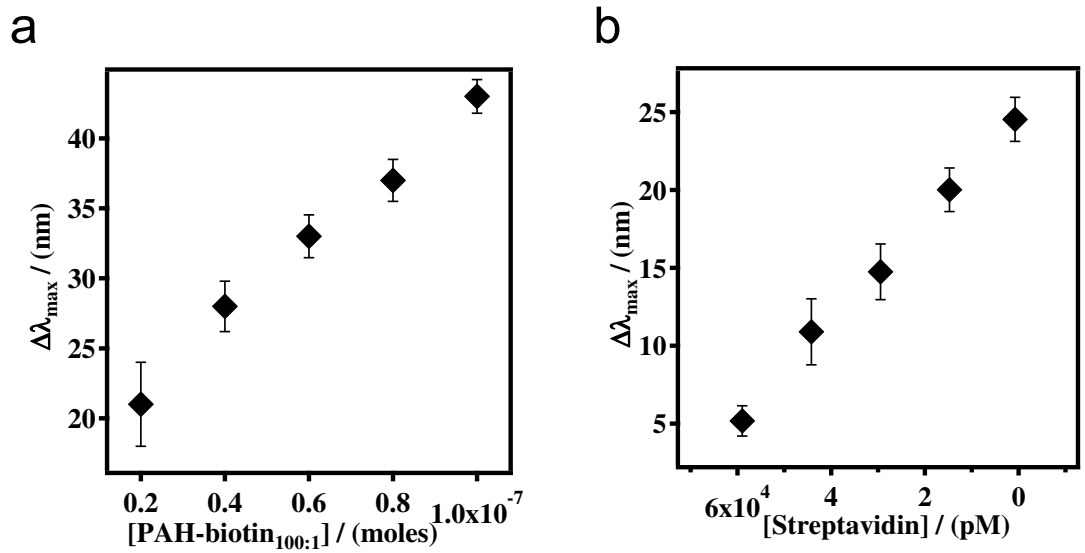

Figure 13. Cumulative shift of etalon's m = 3 reflectance spectra with different amounts of (a) PAH-biotin$_{100:1}$ (b) streptavidin added to PAH–biotin$_{100:1.}$ The pNIPAm-co-AAc microgel-based etalon was soaked in pH 7.2 throughout the experiment, while the temperature was maintained at 25^{o}C. Each point represents the average of at least three independent measurements, and the error

bars are standard deviation for those values. Reprinted with the permission of [59] Copyright © 2013, Elsevier.

Many groups have investigated novel stimuli-responsive polymer based biosensing systems for detection of proteins and DNA.[60-62] As mentioned above, pNIPAm based microgels can be modified with a variety of functional groups that can be incorporated into our optical devices to sense various targets, such as glucose, proteins, and DNA.[48, 51] For example, poly (N-isopropylacrylamide-co-N-(3-aminopropyl) methacrylamide hydrochloride) (pNIPAm-co-APMAH) microgels were synthesized via temperature ramp, surfactant-free, free radical precipitation polymerization.[52, 63] PNIPAm-co-APMAH microgels are positively charged at pH 7.2, and when negatively charged DNA is added to the etalon composed of these positively charged microgels, the microgels are crosslinked and collapsed due to electrostatics and the devices exhibit a spectral shift, as shown in Figure 14. The sensing scheme is shown in Figure 15.

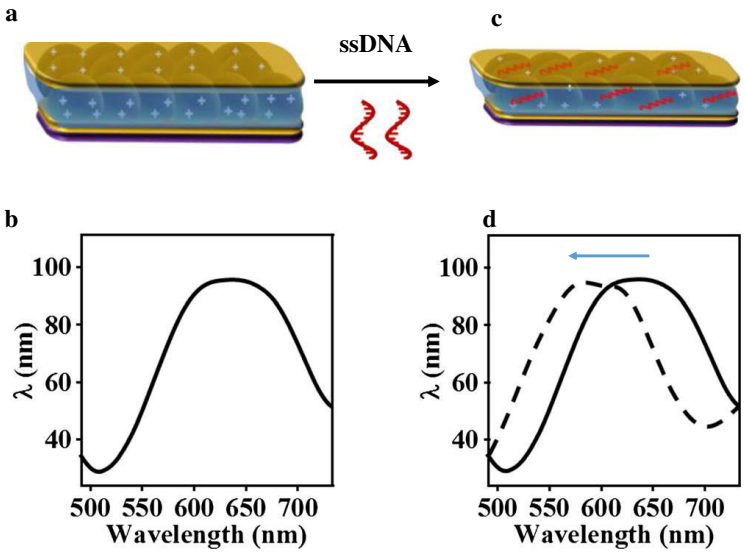

Figure 14. a, The basic structure of pNIPAm-co-N-(3-aminopropyl) methacrylamide hydrochloride microgel-based etalon; b, A schematic representation of a single reflectance peak. Here, the microgels are positively charged in water with a pH <10.0; c, After addition of ssDNA, the

microgels were crosslinked and collapsed, reducing the distance between the two Au layers of the device; d, The peaks (in this case, we show a single peak) of the reflectance spectrum shift to a shorter wavelength. Reprinted with the permission of [52] Copyright © 2014, SpringerVerlag Berlin Heidelberg.

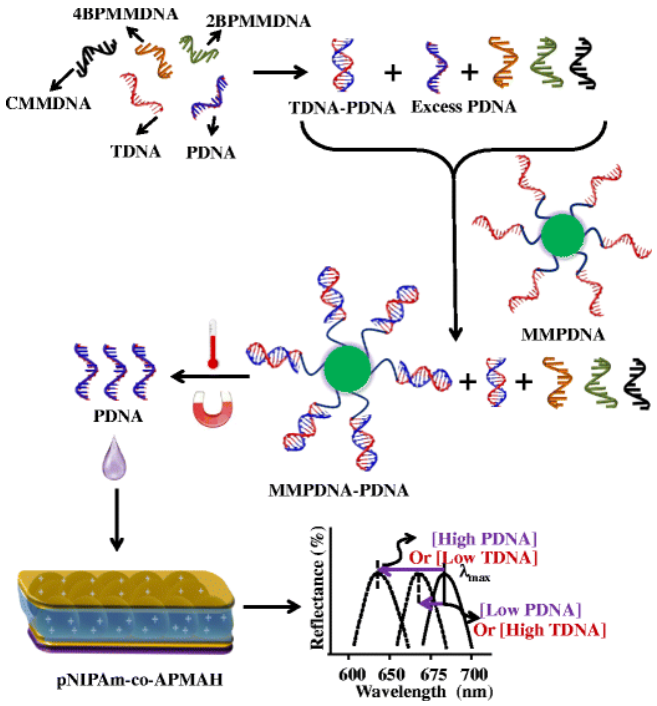

Figure 15. The protocol used for indirectly sensing target DNA (TDNA), by sensing probe DNA (PDNA). The concept is similar to that in Figure 12, except in this case excess PDNA can be related to TDNA concentration, even in the presence of DNA that is completely noncomplementary to PDNA (CMMDNA), and with 2 and 4 base pair mismatches (2BPMMDNA and 4BPMMDNA). Reprinted with the permission of [52] Copyright © 2014, SpringerVerlag Berlin Heidelberg.

Specifically, as can be seen in Figure 15, an excess amount of PDNA is exposed to a solution containing TDNA and DNA with a completely mismatched sequence (CMMDNA), and DNA with four (4BPMMDNA) and two base mismatches (2BPMMDNA). The PDNA binds the TDNA completely, leaving behind excess, unbound PDNA in solution. Magnetic microparticles

(MMPDNA) that are functionalized with the complete complement to PDNA are added to the solution to capture the excess PDNA. A magnet is then used to isolate the magnetic microparticles bound with PDNA (MMPDNA–PDNA) from the solution. After washing the MMPDNA–PDNA, the PDNA is recovered by heating the solution to melt the DNA off of the MMPDNA–PDNA, and the excess PDNA is recovered and added to the etalon. In this case, a large spectral shift from the etalon corresponds to a large excess of PDNA, which means a low concentration of TDNA was present in the initial solution. The opposite is true as well—a low concentration of PDNA left in solution yields a small spectral shift from the device, meaning there was a large amount of TDNA present in the initial solution. This illustrates the strength of the current system—low concentrations of TDNA yield large spectral shifts making the device more sensitive to low DNA concentrations.

Recently, our group developed novel multiresponsive pNIPAm-based microgels by incorporation of the molecule triphenylmethane leucohydroxide (TPL) into their structure. Figure 16 shows the schematic depiction of TPL-modified microgels and their response to various stimuli. These microgels were subsequently used to fabricate etalons, and the optical properties investigated in response to ultraviolet and visible irradiation, solution pH changes, and the presence of a mimic of the nerve agent Tabun was characterized.[53] We also clearly showed that the optical properties of the device depended dramatically on these stimuli and show great promise for remote actuation and sensing.

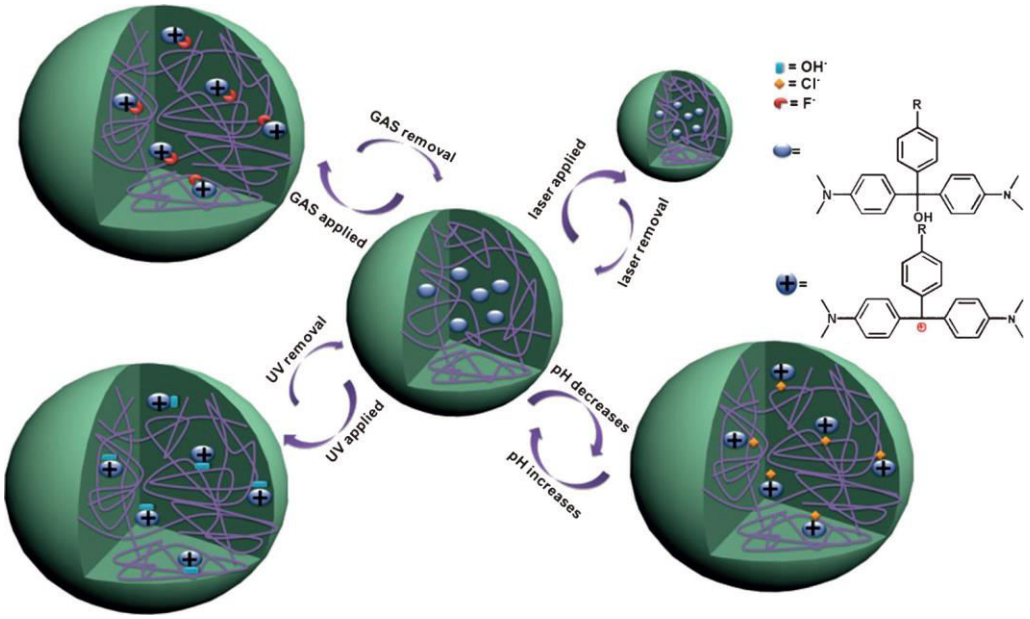

Figure 16. The various responses expected from TPL-modified microgels. The TPL structure is shown on the right. Reprinted with the permission of [53] Copyright © 2014 WILEYVCH Verlag GmbH & Co. KGaA, Weinheim.

Conclusion:

We have briefly reviewed a number of key examples of polymer-based photonic materials as sensors, which primarily relied on their ability to change optical properties in response to different stimuli. In many cases, the optical properties depended on the analyte changing the material's lattice constant and/or its effective refractive index. PNIPAm microgel-based devices were subsequently introduced, and their use as sensors detailed, with a focus on pH, glucose, protein, and DNA sensing. We conclude that pNIPAm microgel-based devices show enormous promise for sensing applications, although more work is needed to enhance the selectivity and sensitivity of the devices. Additionally, there are many challenges that exist to make photonic materials practical for various applications. For example, the tunability of the optical properties of photonic materials depends on the tunability of the material's ordered elements; it also depends on the crystal structure. Therefore, novel materials, and novel photonic material fabrication protocols, are needed to expand their utility

and capabilities. Many different novel self-assembly processes have been developed in the past years to solve the fabrication issues, allowing them to be made more efficiently. As sensors, photonic materials in general need to be made more sensitive and selective, but their response times also need to be minimized. This can be accomplished by altering the materials dimensions, porosity, etc. As a whole, the field is mature, but more advances are needed to bring these very useful materials to the masses.

Acknowledgements:

MJS acknowledges funding from the University of Alberta (the Department of Chemistry and the Faculty of Science), the Natural Sciences and Engineering Research Council of Canada (NSERC), the Canada Foundation for Innovation (CFI), the Alberta Advanced Education & Technology Small Equipment Grants Program (AET/SEGP), Grand Challenges Canada and IC-IMPACTS. YG and XL acknowledge Alberta Innovates Technology Futures (AITF) for graduate student scholarships.

References:

[1] K. L. Hamner, C. M. Alexander, K. Coopersmith, D. Reishofer, C. Provenza, M. M. Maye, *ACS Nano* **2013**, *7*, 7011.
[2] H. Meng, Jinlian Hu, *Journal of Intelligent Material Systems and Structures* **2010**, *21*, 859.
[3] L. Ionov, *Journal of Materials Chemistry* **2010**, *20*, 3382.
[4] N. A. Peppas, J. Z. Hilt, A. Khademhosseini, R. Langer, *Advanced Materials* **2006**, *18*, 1345.
[5] Y. Qiu, K. Park, *Advanced Drug Delivery Reviews* **2001**, *53*, 321.
[6] J. H. Holtz, S. A. Asher, *Nature* **1997**, *389*, 829.
[7] L. E. Bromberg, E. S. Ron, *Advanced Drug Delivery Reviews* **1998**, *31*, 197.
[8] T. Hoare, R. Pelton, *Macromolecules* **2004**, *37*, 2544.
[9] S. Dai, P. Ravi, K. C. Tam, *Soft Matter* **2009**, *5*, 2513.
[10] G. Liu, W. Liu, C.-M. Dong, *Polymer Chemistry* **2013**, *4*, 3431.
[11] I. C. Kwon, Y. H. Bae, S. W. Kim, *Nature* **1991**, *354*, 291.
[12] B. Brugger, W. Richtering, *Advanced Materials* **2007**, *19*, 2973.
[13] G. R. Hendrickson, L. Andrew Lyon, *Soft Matter* **2009**, *5*, 29.
[14] S. Su, M. M. Ali, C. D. M. Filipe, Y. Li, R. Pelton, *Biomacromolecules* **2008**, *9*, 935.
[15] J. K. Oh, D. I. Lee, J. M. Park, *Progress in Polymer Science* **2009**, *34*, 1261.
[16] Y. Gao, G. P. Zago, Z. Jia, M. J. Serpe, *ACS Applied Materials & Interfaces* **2013**, *5*, 9803.

[17] Y. Takashima, S. Hatanaka, M. Otsubo, M. Nakahata, T. Kakuta, A. Hashidzume, H. Yamaguchi, A. Harada, *Nat Commun* **2012**, *3*, 1270.
[18] M. Bassil, M. Ibrahim, M. El Tahchi, *Soft Matter* **2011**, *7*, 4833.
[19] C. E. Reese, A. V. Mikhonin, M. Kamenjicki, A. Tikhonov, S. A. Asher, *Journal of the American Chemical Society* **2004**, *126*, 1493.
[20] Y. Guan, Y. Zhang, *Soft Matter* **2011**, *7*, 6375.
[21] G. Zhang, C. Wu, *Journal of the American Chemical Society* **2001**, *123*, 1376.
[22] C. Wu, S. Zhou, *Macromolecules* **1995**, *28*, 8381.
[23] T. Hoare, R. Pelton, *Macromolecules* **2007**, *40*, 670.
[24] J. Gao, C. Wu, *Macromolecules* **1997**, *30*, 6873.
[25] M. Zhou, J. Xie, S. Yan, X. Jiang, T. Ye, W. Wu, *Macromolecules* **2014**, *47*, 6055.
[26] S. Dhanya, D. Bahadur, G. C. Kundu, R. Srivastava, *European Polymer Journal* **2013**, *49*, 22.
[27] W. Zhang, Z. Mao, C. Gao, *Journal of Colloid and Interface Science* **2014**, *434*, 122.
[28] J. Ge, Y. Yin, *Angewandte Chemie International Edition* **2011**, *50*, 1492.
[29] J. H. Moon, S. Yang, *Chemical Reviews* **2009**, *110*, 547.
[30] F. H. Schacher, P. A. Rupar, I. Manners, *Angewandte Chemie International Edition* **2012**, *51*, 7898.
[31] A. Santos, T. Kumeria, D. Losic, *TrAC Trends in Analytical Chemistry* **2013**, *44*, 25.
[32] S.-i. Shinohara, T. Seki, T. Sakai, R. Yoshida, Y. Takeoka, *Chemical Communications* **2008**, 4735.
[33] R. B. Wehrspohn, J. Üpping, *Journal of Optics* **2012**, *14*, 024003.
[34] S. Domínguez, I. Cornago, O. García, M. Ezquer, M. J. Rodríguez, A. R. Lagunas, J. Pérez-Conde, J. Bravo, *Photonics and Nanostructures - Fundamentals and Applications* **2013**, *11*, 29.
[35] W. Chen, K. D. Long, H. Yu, Y. Tan, J. S. Choi, B. A. Harley, B. T. Cunningham, *Analyst* **2014**, *139*, 5954.
[36] W. Chen, K. D. Long, M. Lu, V. Chaudhery, H. Yu, J. S. Choi, J. Polans, Y. Zhuo, B. A. C. Harley, B. T. Cunningham, *Analyst* **2013**, *138*, 5886.
[37] P. V. Parimi, W. T. Lu, P. Vodo, S. Sridhar, *Nature* **2003**, *426*, 404.
[38] J. M. Weissman, H. B. Sunkara, A. S. Tse, S. A. Asher, *Science* **1996**, *274*, 959.
[39] K. Lee, S. A. Asher, *Journal of the American Chemical Society* **2000**, *122*, 9534.
[40] V. L. Alexeev, A. C. Sharma, A. V. Goponenko, S. Das, I. K. Lednev, C. S. Wilcox, D. N. Finegold, S. A. Asher, *Analytical Chemistry* **2003**, *75*, 2316.
[41] J.-T. Zhang, N. Smith, S. A. Asher, *Analytical Chemistry* **2012**, *84*, 6416.
[42] H. Fudouzi, T. Sawada, *Langmuir* **2005**, *22*, 1365.
[43] E. Lee, J. Kim, J. Myung, Y. Kang, *Macromolecular Research* **2012**, *20*, 1219.
[44] M. Honda, T. Seki, Y. Takeoka, *Advanced Materials* **2009**, *21*, 1801.
[45] M. Karg, T. Hellweg, P. Mulvaney, *Advanced Functional Materials* **2011**, *21*, 4668.
[46] C. D. Sorrell, M. C. D. Carter, M. J. Serpe, *Advanced Functional Materials* **2011**, *21*, 425.
[47] C. D. Sorrell, M. J. Serpe, *Advanced Materials* **2011**, *23*, 4088.
[48] C. Sorrell, M. Serpe, *Analytical and Bioanalytical Chemistry* **2012**, *402*, 2385.
[49] L. Hu, M. J. Serpe, *Journal of Materials Chemistry* **2012**, *22*, 8199.
[50] K. C. C. Johnson, F. Mendez, M. J. Serpe, *Analytica Chimica Acta* **2012**, *739*, 83.
[51] M. R. Islam, M. J. Serpe, *Chemical Communications* **2013**, *49*, 2646.
[52] M. Islam, M. Serpe, *Analytical and Bioanalytical Chemistry* **2014**, *406*, 4777.
[53] Q. M. Zhang, W. Xu, M. J. Serpe, *Angewandte Chemie International Edition* **2014**, *53*, 4827.
[54] W. Xu, Y. Gao, M. J. Serpe, *Journal of Materials Chemistry C* **2014**, *2*, 3873.
[55] L. Hu, M. J. Serpe, *Chemical Communications* **2013**, *49*, 2649.
[56] M. R. Islam, K. C. C. Johnson, M. J. Serpe, *Analytica Chimica Acta* **2013**, *792*, 110.
[57] M. R. Islam, M. J. Serpe, *Macromolecules* **2013**, *46*, 1599.
[58] M. R. Islam, M. J. Serpe, *APL Materials* **2013**, *1*.
[59] M. R. Islam, M. J. Serpe, *Biosensors and Bioelectronics* **2013**, *49*, 133.

[60] T. A. Taton, C. A. Mirkin, R. L. Letsinger, *Science* **2000**, *289*, 1757.
[61] Y. Zhao, X. Zhao, B. Tang, W. Xu, J. Li, J. Hu, Z. Gu, *Advanced Functional Materials* **2010**, *20*, 976.
[62] M. Gao, K. Gawel, B. T. Stokke, *Soft Matter* **2011**, *7*, 1741.
[63] M. R. Islam, M. J. Serpe, *Analytica Chimica Acta* **2014**, *843*, 83.